Available online at www.sciencedirect.com

ScienceDirect

IFAC Papers Online
CONFERENCE PAPER ARCHIVE

IFAC-PapersOnLine 49-18 (2016) 704–709

Extending Data-Driven Koopman Analysis to Actuated Systems

Matthew O. Williams * **Maziar S. Hemati** **
Scott T. M. Dawson *** **Ioannis G. Kevrekidis** ****,†
Clarence W. Rowley ‡

* *United Technologies Research Center, East Hartford, CT 06118 USA (e-mail:william1@utrc.utc.com)*
** *Department of Aerospace Engineering and Mechanics, University of Minnesota, Minneapolis, MN, 55455 USA (e-mail: mhemati@umn.edu)*
*** *Department of Mechanical and Aerospace Engineering, Princeton University, Princeton, NJ 08544 USA (e-mail: stdawson@princeton.edu)*
**** *Department of Chemical and Biological Engineering & PACM, Princeton University, Princeton, NJ 08544 USA (e-mail: yannis@princeton.edu)*
† *Institute for Advanced Study, Technische Universität München, Garching, Germany*
‡ *Department of Mechanical and Aerospace Engineering, Princeton University, Princeton, NJ 08544 USA (e-mail: cwrowley@princeton.edu)*

Abstract: In recent years, methods for data-driven Koopman spectral analysis, such as Dynamic Mode Decomposition (DMD), have become increasingly popular approaches for extracting dynamically relevant features from data sets. However to establish the connection between techniques like DMD or Extended DMD (EDMD) and the Koopman operator, assumptions are made about the nature of the supplied data. In particular, both methods assume the data were generated by an autonomous dynamical system, which can be limiting in certain experimental or computational settings, such as when system actuation is present. We present a modification of EDMD that overcomes this limitation by compensating for the effects of actuation, and is capable of recovering the leading Koopman eigenvalues, eigenfunctions, and modes of the unforced system. To highlight the efficacy of this approach, we apply it to two examples with (quasi)-periodic forcing: the first is the Duffing oscillator, which demonstrates eigenfunction approximation, and the second is a lattice Boltzmann code that approximates the FitzHugh-Nagumo partial differential equation and shows Koopman mode and eigenvalue computation.

Keywords: nonlinear theory, nonlinear analysis, Koopman operator, model reduction, system identification, data processing

1. INTRODUCTION

In many applications, tasks such as parameter optimization or controller design become infeasible in practice due to the computational cost associated with system simulation. One method for avoiding this computational issue is to construct an accurate reduced order model for the system dynamics. Although there are many methods for accomplishing this task, data-driven approaches like the Proper Orthogonal Decomposition-Galerkin (POD-Galerkin) method, Vector Autoregressive models, or Linear Parameter Varying (LPV) models have become popular due to the availability of data and efficient algorithms (see, e.g., Holmes et al. (1998), Lütkepohl (2005), and Bachnas et al. (2014)).

One subset of these techniques are methods based on the analysis of the Koopman operator (see Budišić et al. (2012), Mezič (2013), and the references therein), which governs the evolution of scalar observables of the system state. The Koopman operator provides a principled and often globally valid framework that trades dimensionality for linearity; more precisely, the Koopman operator is an infinite-dimensional *linear* operator that can describe the dynamics of a finite-dimensional *nonlinear* system. Because it is a linear operator, one can define Koopman *eigenvalues*, *eigenfunctions*, and *modes*, which can be useful aids in understanding possible system behaviors, generating dynamically interpretable low-dimensional embeddings of high-dimensional state spaces, and visualizing coherent structures and patterns in the underlying system. Furthermore, using techniques such as Dynamic Mode Decomposition (DMD), first proposed by Schmid (2010), or the related Extended DMD (EDMD) proposed in Williams

10.1016/j.ifacol.2016.10.248

et al. (2015b), it is often possible to approximate a few of the leading Koopman eigenvalues, eigenfunctions and modes directly from data (see, e.g., Rowley et al. (2009), Tu et al. (2014), and Williams et al. (2015b)).

Because they are strictly data-driven, DMD and EDMD will produce results for any appropriately formatted set of data, but connecting these outputs to the Koopman operator requires additional knowledge about the nature of the data supplied. In particular, for the arguments used by Williams et al. (2015b) to be valid, the snapshot pairs must have been generated by an autonomous dynamical system. However, this restriction does not hold for all data or dynamical systems; one common example is when system actuation is used to explore state space during the data collection process. As we will demonstrate in this manuscript, the presence of actuation can deleteriously impact the results of methods like EDMD, and if not taken into consideration, destroy their connection with the Koopman operator.

To address this issue, we present a modification of EDMD designed to compensate for the effects of this actuation, and reestablishing the connection between EDMD and the Koopman operator of the underlying dynamical system for this more general class of data sets. This work draws upon a number of sources including system identification methods for LPV models and existing extensions of DMD such as Proctor et al. (2014). Our contribution is combining these techniques into a single computational procedure and establishing its connection with the Koopman operator. Although the computational cost of this procedure is greater than that of Proctor et al. (2014), it can accurately reproduce a larger class of Koopman eigenfunctions provided the dictionary elements are chosen appropriately.

The remainder of the paper is outlined as follows: the computational procedure and associated theory are given in Sec. 2, which is followed by two illustrative examples. In Sec. 3, we apply the approach to the Duffing oscillator with periodic forcing where the Koopman eigenfunctions are of interest. In Sec. 4, we apply the method to data from a lattice Boltzmann model of the FitzHugh-Nagumo equation subject to quasi-periodic forcing, which is a higher dimensional example where the modes and eigenvalues are desired. Finally, concluding remarks and future outlook are presented in Sec. 5.

2. THEORY AND COMPUTATIONAL PROCEDURE

In this section, we present a modification of Extended DMD (EDMD) that compensates for system actuation. To provide some background for the approach, we review a few of the salient properties of the Koopman operator and "standard" EDMD before outlining our method. We refer the reader to Budišić et al. (2012), Mezič (2013), and the references contained therein for more information about the underlying theory, and Tu et al. (2014), Williams et al. (2015b), and the references therein for more information about DMD and EDMD respectively.

2.1 The Koopman Operator

For the purposes of this manuscript, the Koopman operator, $\mathcal{K}$, is defined for the autonomous, discrete time, and deterministic dynamical system given by the triple $(n, \mathcal{M}, \boldsymbol{F})$, where $n \in \mathbb{Z}$ is time, $\mathcal{M} \subseteq \mathbb{R}^N$ is state space, and $\boldsymbol{F} : \mathcal{M} \to \mathcal{M}$ is the evolution law. However, $\mathcal{K}$ acts on scalar observables, $\psi : \mathcal{M} \to \mathbb{C}$ rather than states. In particular, the action of the Koopman operator is

$$(\mathcal{K}\psi)(\boldsymbol{x}) = (\psi \circ \boldsymbol{F})(\boldsymbol{x}) = \psi(\boldsymbol{F}(\boldsymbol{x})), \tag{1}$$

and is therefore often referred to as the *composition operator* as it composes a scalar observable with the evolution law. Intuitively, $\mathcal{K}$ takes a scalar function ψ and returns a new function $\mathcal{K}\psi$ that predicts what the value of ψ will be "one time step" in the future.

Because it acts on functions rather than states, the Koopman operator is infinite dimensional even if state space is finite dimensional. The benefit, however, is that it is a *linear operator even if the underlying system is nonlinear*. Because it is linear, the Koopman operator can have eigenvalues (μ_i) and eigenfunctions (φ_i), which satisfy

$$\mathcal{K}\varphi_i = \mu_i \varphi_i. \tag{2}$$

In addition to these intrinsic quantities, the Koopman operator also has *modes* $(\boldsymbol{v}_i)$, which are defined for a given *vector valued observable*, say, $\boldsymbol{g} : \mathcal{M} \to \mathbb{R}^M$. Taken together the eigenfunctions, eigenvalues, and modes allow a vector valued observable m-steps in the future to be written as:

$$\boldsymbol{g}(\boldsymbol{F}^{(m)}(\boldsymbol{x})) = \sum_{i=1}^{\infty} \mu_i^m \boldsymbol{v}_i \varphi_i(\boldsymbol{x}), \tag{3}$$

where $\boldsymbol{F}^{(m)}(\boldsymbol{x})$ denotes m applications of the map $\boldsymbol{F}$ to the state $\boldsymbol{x}$. It should be noted that not all vector valued observables can be written in the form shown in (3), and for some systems or observables, additional terms to account for the remainder of the spectrum of the Koopman operator may be required as shown by Mezič (2013).

2.2 Extended Dynamic Mode Decomposition

Extended DMD approximates the Koopman operator using a "pragmatic" weighted residual method. Similar to "standard" weighted residual methods, we assume that a scalar observable of interest can be written as the linear superposition of dictionary elements ψ_i:

$$\phi(\boldsymbol{x}) = \sum_{i=1}^{M} a_i \psi_i(\boldsymbol{x}), \tag{4}$$

where the a_i are the coefficients in the expansion. We refer to ψ_i as a *dictionary element* rather than a *basis function* because it is often unclear whether or not the ψ_i are linearly independent with respect to the state space of the underlying dynamical system. The action of $\mathcal{K}$ on ϕ results in another scalar observable

$$(\mathcal{K}\phi)(\boldsymbol{x}) = \sum_{i=1}^{M} b_i \psi_i(\boldsymbol{x}) + r(\boldsymbol{x}), \tag{5}$$

with different coefficients, b_i, and the function r, which is the residual that appears because the M-dimensional subspace of scalar observables used in this approximation may not be closed with respect to the action of the Koopman operator.

In a weighted residual method, a finite-dimensional approximation of an infinite dimensional operator, which we refer to here as $\boldsymbol{K}$, is achieved by taking inner products with a set of M weight functions, which we refer to as W_m

for $m = 1, \ldots, M$. The matrix that minimizes the residual given these weight functions is

$$\boldsymbol{K} \triangleq {\boldsymbol{\Psi_X}}^{+}\boldsymbol{\Psi_Y}, \tag{6}$$

where the ij-th elements of $\boldsymbol{\Psi_X}, \boldsymbol{\Psi_Y} \in \mathbb{R}^{M\times M}$ are ${\boldsymbol{\Psi_X}}^{(ij)} = \langle W_i, \psi_j \rangle$ and ${\boldsymbol{\Psi_Y}}^{(ij)} = \langle W_i, \mathcal{K}\psi_j \rangle$ respectively, and $+$ denotes the Moore-Penrose pseudoinverse. There are many ways to choose the weight functions, but most relevant here are collocation methods, which choose $W_i(\boldsymbol{x}) = \delta(\boldsymbol{x} - \boldsymbol{x}_i)$ where $\boldsymbol{x}_i$ is a pre-determined collocation point (see, e.g., Boyd (2001)).

Extended DMD does not require $\boldsymbol{F}$ to be available explicitly, but it does need a data set of snapshots pairs:

$$\{(\boldsymbol{x}_m, \boldsymbol{y}_m)\}_{m=1}^{M}, \text{ where } \boldsymbol{y}_m = \boldsymbol{F}(\boldsymbol{x}_m), \tag{7}$$

which contain information about the action of $\boldsymbol{F}$. Due to the lack of explicit governing equations, we cannot evaluate the inner products needed to compute $\boldsymbol{\Psi_Y}$ and $\boldsymbol{\Psi_X}$ for most choices of weight functions. However, one *pragmatic* choice is to let $W_i(\boldsymbol{x}) = \delta(\boldsymbol{x} - \boldsymbol{x}_i)$ where $\boldsymbol{x}_i$ is the i-th snapshot in the data set. With this choice, the elements of $\boldsymbol{\Psi_X}$ and $\boldsymbol{\Psi_Y}$ are:

$${\boldsymbol{\Psi_X}}^{(ij)} = \psi_j(\boldsymbol{x}_i), \quad {\boldsymbol{\Psi_Y}}^{(ij)} = (\mathcal{K}\psi_j)(\boldsymbol{x}_i) = \psi_j(\boldsymbol{y}_i), \tag{8}$$

or the dictionary elements evaluated at each of the $\boldsymbol{x}_i$ and its image $\boldsymbol{y}_i$. As a result, EDMD is a collocation method, where the collocation points were chosen solely so that the inner products can be evaluated.

The advantage of this interpretation is that the relationship between $\boldsymbol{K}$ and $\mathcal{K}$ is clear. In particular, the eigenvalues of $\boldsymbol{K}$ are approximations of some of the eigenvalues of $\mathcal{K}$. Furthermore, the right eigenvectors of $\boldsymbol{K}$ help to approximate the eigenfunctions of $\mathcal{K}$. If $\boldsymbol{a}_i$ is the i-th eigenvector of $\boldsymbol{K}$ with the eigenvalues μ_i, then the approximation of the i-th eigenfunction is

$$\varphi_i(\boldsymbol{x}) = \sum_{m=1}^{M} \boldsymbol{a}_i^{(m)} \psi_m(\boldsymbol{x}), \tag{9}$$

where $\boldsymbol{a}_i^{(m)}$ is the m-th element of the eigenvector. Similarly, if $\boldsymbol{w}_i$ is the i-th *left eigenvector* of $\boldsymbol{K}$, then the approximation of the i-th Koopman mode is:

$$\boldsymbol{v}_i = \sum_{m=1}^{M} \hat{\boldsymbol{x}}_m \boldsymbol{w}_i^{(m)}, \tag{10}$$

where $\hat{\boldsymbol{x}}_m$ is the m-th column of

$$[\hat{\boldsymbol{x}}_1 \ \hat{\boldsymbol{x}}_2 \ \cdots \ \hat{\boldsymbol{x}}_M] \triangleq [\boldsymbol{g}(\boldsymbol{x}_1) \ \cdots \ \boldsymbol{g}(\boldsymbol{x}_M)] \, ({\boldsymbol{\Psi_X}}^{T})^{+} \tag{11}$$

where $\boldsymbol{g}$ is the vector-valued observable whose modes are desired, and $\boldsymbol{x}_m$ is the m-th snapshot.

2.3 Compensating for System Actuation

To compensate for inputs, we combine EDMD with techniques used to identify linear parameter varying (LPV) models (see Bachnas et al. (2014) and the references therein) to obtained a parameter varying approximation of the Koopman operator. An LPV representation was chosen because the Koopman operator is a linear operator, so the LPV assumption of linear dynamics is satisfied, but could have complex and possible nonlinear dependence on the system parameters. Typically, LPV models treat system parameters and inputs separately (e.g., using standard state-space notation, they identify the matrices $\boldsymbol{A}(\boldsymbol{p})$ and $\boldsymbol{B}(\boldsymbol{p})$ where $\boldsymbol{p}$ are the system parameters, which characterize the unforced dynamics and response to actuation respectively). Our analysis focuses on identifying *the Koopman operator of an underlying unforced system* from data obtained with actuation, so inputs will be lumped in with the parameters, and our approach will not compute an analog of $\boldsymbol{B}(\boldsymbol{p})$. The analysis and effective computation of *the Koopman operator for a forced dynamical system* is currently an area of active research, and beyond the scope of this manuscript.

In what follows, the data now comes in *triples*,

$$\{(\boldsymbol{x}_m, \boldsymbol{u}_m, \boldsymbol{y}_m)\}_{m=1}^{M} \text{ where } \boldsymbol{y}_m = \boldsymbol{F}(\boldsymbol{x}_m, \boldsymbol{u}_m). \tag{12}$$

As before, we assume the space of observables is approximated using a finite set of dictionary elements of the form shown in (4) and (5), which do not have a direct dependence on the system inputs. However, the *mapping* between observables will, so we seek a parameter-dependent matrix that minimizes:

$$\min_{\boldsymbol{K}} \frac{1}{2} \sum_{m=1}^{M} \|{\boldsymbol{\Psi_Y}}^{(m)} - {\boldsymbol{\Psi_X}}^{(m)} \boldsymbol{K}(\boldsymbol{u}^{(m)})\|^2, \tag{13}$$

where ${\boldsymbol{\Psi_X}}^{(m)}$, ${\boldsymbol{\Psi_Y}}^{(m)}$, and $\boldsymbol{u}^{(m)}$ denote the m-th row of the matrix. As shown above by the form of $\boldsymbol{K}$, this framework treats *the inputs as time-varying system parameters* and not as control parameters. To include parameters, we expand the entries in terms of a set of N_u basis functions:

$$\boldsymbol{K} = \sum_{n=1}^{N_u} \tilde{\psi}_n(\boldsymbol{u}) \boldsymbol{K}_n, \tag{14}$$

where $\boldsymbol{K_n}$ is the n-th coefficient in the expansion, and $\tilde{\psi}_n$ is the n-th basis function that maps *inputs* to scalars. For the sinusoidal forcing terms in the examples that follow, only a few of these functions were required to accurately approximate the leading Koopman eigenfunctions, but more complex forcing terms may require larger numbers. As with the ψ_m, the $\tilde{\psi}_n$ must be chosen by the user, and the optimal choice is likely dependent on both the underlying system and the type of forcing used to generate the data. Then, we substitute (14) into (13) and solve for the $\boldsymbol{K}_n$ using:

$$\min_{\boldsymbol{K}} \frac{1}{2} \sum_{m=1}^{M} \|{\boldsymbol{\Psi_Y}}^{(m)} - \sum_{n=1}^{N_u} \tilde{\psi}_n(\boldsymbol{u}^{(m)}) {\boldsymbol{\Psi_X}}^{(m)} \boldsymbol{K}_n\|^2. \tag{15}$$

For notational convenience, we define the matrix $\boldsymbol{\Psi_{XU}}$ where the m-th row of the matrix is

$${\boldsymbol{\Psi_{XU}}}^{(m)} \triangleq [\tilde{\psi}_1(\boldsymbol{u}^{(m)}) {\boldsymbol{\Psi_X}}^{(m)}, \tilde{\psi}_2(\boldsymbol{u}^{(m)}) {\boldsymbol{\Psi_X}}^{(m)}, \cdots], \tag{16}$$

and the matrix

$$\hat{\boldsymbol{K}} \triangleq \begin{bmatrix} \boldsymbol{K}_1 \\ \boldsymbol{K}_2 \\ \vdots \\ \boldsymbol{K}_{N_u} \end{bmatrix}. \tag{17}$$

Using these quantities, (15) becomes

$$\min_{\hat{\boldsymbol{K}}} \frac{1}{2} \|\boldsymbol{\Psi_Y} - \boldsymbol{\Psi_{XU}} \hat{\boldsymbol{K}}\|_F^2, \tag{18}$$

which has the solution $\hat{\boldsymbol{K}} = {\boldsymbol{\Psi_{XU}}}^{+} \boldsymbol{\Psi_Y}$. Given $\hat{\boldsymbol{K}}$, we can compute $\boldsymbol{K}$ at a given value of $\boldsymbol{u}$ using (14), and given $\boldsymbol{K}$ the eigenvalues, eigenfunctions, and modes can be approximated using (9) and (10).

In practice, EDMD has the tendency to over-fit the data supplied to it, and this approach, which will increase the

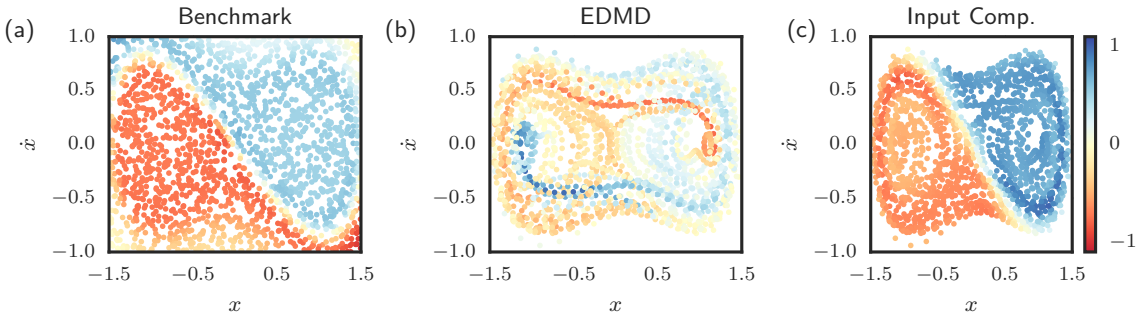

Fig. 1. The value of leading non-trivial Koopman eigenfunction of Duffing oscillator at the 2000 data points used to approximate it. The reference case is presented in (a), where the initial points were chosen from a uniform distribution, and the level sets of the eigenfunction reveal the two basins of attraction in this problem. In (b), EDMD is applied to actuated data *without input compensation*, and the leading eigenfunction is clearly different from the benchmark. In (c), EDMD with input compensation is used, and recovers an eigenfunction that is, once again, effective at partitioning state space into basins of attraction. All three functions were normalized such that their maximum amplitude is one in the window shown.

number of degrees of freedom, can exacerbate this issue. In an effort to avoid this, we regularize based on the $L_{1,2}$ norm, which results in the optimization problem:

$$\min_{\hat{\boldsymbol{K}}} \frac{1}{2}\|\boldsymbol{\Psi_Y} - \boldsymbol{\Psi_{XU}}\hat{\boldsymbol{K}}\|_F^2 + \gamma\|\hat{\boldsymbol{K}}\|_{1,2}, \tag{19}$$

where

$$\|\hat{\boldsymbol{K}}\|_{1,2} \triangleq \sum_{m=1}^{M}\sqrt{\sum_{n=1}^{N}\hat{\boldsymbol{K}}_{mn}^2}, \tag{20}$$

and γ is a regularization parameter. This type of regularization is the *group lasso penalty*, which in this context, encourages $\hat{\boldsymbol{K}}$ to have a small number of nonzero rows. Because each row contains the coefficients associated with one dictionary element, this form of regularization identifies a small set of functions that are useful for predicting the evolution of *many* scalar observables (see Yuan and Lin (2006)). Furthermore, the resulting problem can be solved efficiently using the Alternating Direction Method of Multipliers (ADMM) as described by Boyd et al. (2011). Because it is iterative, this approach is more computationally expensive than EDMD or DMD, but appears to be more robust to the choice of dictionary elements and their associated parameters for the two examples that follow.

3. EXAMPLE I: THE DUFFING OSCILLATOR

The first example we present is the Duffing oscillator, which we will use to demonstrate the effects that system inputs can have on the approximation of the leading Koopman eigenfunctions. The governing equations are:

$$\ddot{x} + \delta\dot{x} + \beta x + \alpha x^3 = u(t), \tag{21}$$

where $u(t) = a\cos(\omega t)$, $\alpha = 1$, $\beta = -1$, and $\delta = 0.2$. For these parameter values, the Duffing oscillator has two stable spirals at $x = \pm 1$ and $\dot{x} = 0$ with non-trivial basins of attraction. In our benchmark data set, we set $a = 0$ and construct a data set using 2000 randomly but uniformly distributed initial conditions for $x, \dot{x} \in (-1.5, 1.5)$. Then we run a single trajectory consisting of 2001 steps with $a = 0.3$ and $\omega = 1$ starting at $x = \dot{x} = 0$, which explores a similar subset of state space but violates the assumption of autonomy. The data in both experiments are sampled at $\Delta t = 0.25$, and the set of scalar observables are exponential radial basis functions:

$$\psi_i(\boldsymbol{x}) = \exp\left(\frac{-\|\boldsymbol{x} - \boldsymbol{x}_i\|}{5}\right), \tag{22}$$

where $\boldsymbol{x}_i$ is the i-th element in the data set. Equation 19 was solved with $\gamma = 10^{-4}$ using 200 steps of the ADMM. For the input corrected version, we used a polynomial expansion with $\tilde{\psi}_1(u) = 1$ and $\tilde{\psi}_2(u) = u$.

Figure 1a shows the reference solution obtained by applying EDMD to the autonomous data set. In principle, the eigenvalue associated with this eigenfunction should be unity, and the level sets should indicate the basins of attraction in this problem. Because this is a data-driven approximation, the numerically computed eigenvalue is $\mu = 1.003$, and the numerically obtained eigenfunction takes on a continuum of values rather than two distinct values that cleanly denote basins of attraction. Despite these limitations, the data can be partitioned into two sets using the value of the numerically computed eigenfunctions, as is clearly indicated by the red and blue regions in the figure, which indicate positive and negative eigenfunction values respectively. The dividing point is the zero level set, which appears as yellow in the figure, and correctly assigns 1911 of the 2000 data points (roughly 95% of the data) to the appropriate basin of attraction. Most of the error is due to points on the boundary between the two sets or at the top-right or bottom-left corners of the domain shown in Fig. 1a where many of the initial points leave the domain of interest during the sampling interval.

Now we consider the actuated data set, and apply EDMD with and without input correction. Without compensation for actuation, the eigenvalue closest to unity that is not associated with a constant eigenfunction is $\mu = 0.961$, whose corresponding eigenfunction is shown in Fig. 1b. This eigenfunction has no connection with the one shown in Fig. 1a, so although the eigenvalues appear promising, the results are not meaningful in this case.

On the other hand, Fig. 1c shows the Koopman eigenfunction associated with the eigenvalue $\mu = 0.997$ computed using the same data with input compensation. The most important change is that the eigenfunction agrees with Fig. 1a, and assigns 1963 of the 2000 data points (roughly 98% of the data) to the correct basin. Note that the performance here is better than the reference case because

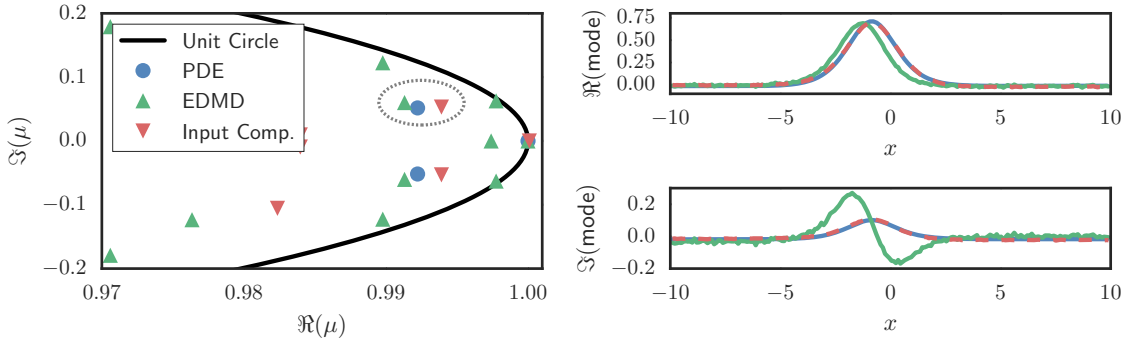

Fig. 2. (left) The numerically computed Koopman eigenvalues for the FitzHugh-Nagumo equation obtained: (green) using EDMD without input compensation, (red) using EDMD with input compensation, and (blue) via direct computation performed on the underlying PDE. (right) The real and imaginary parts of the numerically obtained Koopman modes associated with eigenvalues in the dashed circle where the color of the line corresponds to the color of the markers in the leftmost plot. The imaginary part of the mode highlights the difference between the true Koopman modes and those predicted by EDMD without input compensation.

several of the more "difficult" subsets of state space are not contained within this data set.

There are quantitative differences between these functions: for instance, there is more variance in the value of the eigenfunction within a basin of attraction. These differences are expected; input compensation introduces new degrees of freedom and makes additional assumptions about the parametric dependence of the Koopman operator, all of which could negatively impact the accuracy of the method. However, the purpose of this example is to demonstrate that the nature of the data impacts the validity of the resulting analysis: using "standard" EDMD, our results were useless for the intended task, but by compensating for actuation, we were successful in extracting an eigenfunction that allowed meaningful conclusions to be drawn.

4. EXAMPLE II: A LATTICE BOLTZMANN MODEL FOR THE FITZHUGH-NAGUMO EQUATION

In many application areas, the Koopman modes and eigenvalues are more useful than the Koopman eigenfunctions because they identify coherent patterns in the underlying system associated with a single complex frequency. The modes and eigenvalues "act" like the eigenvalues and eigenvectors of a linear system, but are defined for a broader class of problems including nonlinear systems of ODEs or PDEs as well as agent-based models and mesoscopic models that track densities of heterogeneous agents.

In this example, we consider a mesoscopic lattice-Boltzmann (LB) approximation of the FitzHugh-Nagumo PDE, which is a prototypical example of a reaction diffusion system and sometimes used as a simple model for signal propagation in an axon. The system state of the FHNE is comprised of two fields: v the activator complex and w the inhibitor complex, which evolve according to:

$$\partial_t v = \partial_{xx} v + v - v^3 + w + u(t) e^{-x^2/2}, \tag{23a}$$
$$\partial_t w = \delta \partial_{xx} w + \epsilon(v - a_1 w - a_0), \tag{23b}$$

where $\delta = 4$, $\epsilon = 0.03$, $a_1 = 2$, and $a_0 = -0.03$ on the domain $x \in (-10, 10)$ with Neumann boundary conditions in what follows. For this example, we introduced a forcing term that contains the input:

$$u(t) = 0.005 \left[\cos\left(\frac{2\pi t}{100}\right) + \cos\left(\frac{t}{200}\right) \right], \tag{24}$$

which was chosen so that the forcing periods are incommensurate but on the order of the natural timescales of the problem. Given (23) and data obtained with $u = 0$, Williams et al. (2015a) computed approximations of the leading Koopman eigenvalues and modes that agreed favorably with analytical results such as the ones presented by Gaspard and Tasaki (2001), so EDMD is known to be effective for this problem.

This example builds upon that work in two ways: (i) the introduction of the forcing term in (24), and (ii) the obfuscation of the system state through the use of a lattice-Boltzmann model. The LB model we implement is described in Van Leemput et al. (2005), and consists of six interacting species of particles confined to $N_l = 200$ lattice points. At the n-th lattice point, these species are:

$$\{v_{-1}^{(n)}, v_0^{(n)}, v_1^{(n)}, w_{-1}^{(n)}, w_0^{(n)}, w_1^{(n)}\}, \tag{25}$$

where $v_i^{(n)}$ and $w_i^{(n)}$ are the two different types of reactants. The subscript denotes the velocity of the particles, which for $v_i^{(n)}$ is given by $i\frac{\Delta x}{\Delta t}$, where $i = -1, 0, 1$ where $\Delta x = 0.1$, $\Delta t = 10^{-3}$, and halfway bounce back boundary conditions (no-flux) are imposed at the edges of the lattice. The evolution laws are chosen so that the densities:

$$v^{(n)} \triangleq v_{-1}^{(n)} + v_0^{(n)} + v_1^{(n)}, \quad w^{(n)} \triangleq w_{-1}^{(n)} + w_0^{(n)} + w_1^{(n)}, \tag{26}$$

evolve according to the FHNE with the listed parameters.

The data set consists of 2000 snapshot pairs, where each snapshot is a vector $\mathbb{R}^{1200}$ generated by "stacking" the densities of the six species into a single vector. The sampling interval is $\Delta T = 1$, which is every 1000 steps of the lattice Boltzmann code. The dictionary elements consists of Gaussian radial basis functions,

$$\psi_i(\boldsymbol{x}) = \exp\left(-20\|\boldsymbol{x} - \boldsymbol{x}_i\|^2\right), \tag{27}$$

where $\boldsymbol{x}_i$ is the i-th snapshot in the data set. The parameter dependence is approximated using polynomials up to third order, and the regularization parameter in (19) was chosen to be $\gamma = 10^{-3}$, and 200 iterations of the ADMM appeared to be sufficient to find a solution.

The left plot in Fig. 2 shows the EDMD eigenvalues obtained from this data with and without input correction.

Due to the forcing, the leading uncorrected eigenvalues are effectively on the unit circle, which is indicative of a quasi-periodic orbit or limit cycle. Input compensation "shifts" the eigenvalues away from the unit circle, and with this choice of observables, accurately reproduces the first two layers of the "pyramid" of eigenvalues associated with a stable spiral (see, e.g., Gaspard and Tasaki (2001)). Furthermore, the numerically computed eigenvalues of $\mu = 0.993 \pm 0.053i$ compares favorably with the directly computed values of $\mu \approx 0.992 \pm 0.057i$, which was obtained by linearizing a spectral approximation of the PDE in (23) about the fixed point without forcing.

In addition to extraneous eigenvalues, the forcing term also affects the modes obtained by EDMD. In particular, we focus on the mode for v as defined in (26) associated with the circled eigenvalues in Fig. 2, which are the eigenvalues closest to the true value. Because the eigenvalues are complex, the Koopman mode is part of a complex conjugate pair, so to facilitate comparison, we normalized each mode and chose the phase such that sum of the imaginary part is zero. As shown in the figure, the real parts of both modes have the same mode shape, but there are clear qualitative differences in the imaginary parts of the mode obtained using "standard" EDMD. In particular, the mode obtained without input correction has a zero near $x = 0$, which is near where both the true and corrected modes have their maximums. As a result, system actuation also can have an effect on the eigenvalues and modes, and compensating for inputs can have a visible impact on the quality of the resulting modes and eigenvalues.

5. CONCLUSIONS

In this manuscript, we presented a modification of Extended Dynamic Mode Decomposition designed to mitigate the effects of system actuation, and demonstrated the approach on two illustrative examples. In both cases, the initial results appeared reasonable, but further analysis of the output of EDMD showed clear qualitative differences between the numerically computed and true solutions. Because they are entirely data-driven, methods like DMD or EDMD will produce sets of eigenvalues and their corresponding left- and right-eigenvectors for any set of data. However, interpreting these quantities as Koopman eigenvalues, modes, and eigenfunctions requires additional assumptions to be made; in particular, that the data were generated by an autonomous dynamical system. The failure of "standard" EDMD in the two test cases presented here can be attributed to the violation of this assumption by the introduction of the time-dependent system actuation.

To address this issue, we treated system inputs as a time-varying parameter, and identified a linear parameter varying (LPV) model. As with "standard" EDMD, the user must choose a set of dictionary elements $\psi_i(\boldsymbol{x})$, and to capture the dependence on the inputs, they must also choose a set of functions $\tilde{\psi}_n(\boldsymbol{u})$. Because of these additional degrees of freedom, we introduced $L_{1,2}$ regularization to enhance the robustness of the procedure. This form of regularization would also enhance the robustness of EDMD, but it comes with a significant computational cost due to the iterative nature of the optimization procedure. Although in ideal settings we would use EDMD, obtaining the requisite data sets is not always straightforward or even possible, and in these more realistic settings, methods such as this are necessary to reestablish the connection between methods like DMD or EDMD and the Koopman operator.

ACKNOWLEDGEMENTS

M.O.W. would like to thank Joshua L. Proctor for helpful discussions about DMD for control problems, and acknowledges partial support for the work by NSF DMS-1204783.

REFERENCES

Bachnas, A., Tóth, R., Ludlage, J., and Mesbah, A. (2014). A review on data-driven linear parameter-varying modeling approaches: A high-purity distillation column case study. *Journal of Process Control*, 24, 272–285.

Boyd, J.P. (2001). *Chebyshev and Fourier spectral methods*. Courier Corporation.

Boyd, S., Parikh, N., Chu, E., Peleato, B., and Eckstein, J. (2011). Distributed optimization and statistical learning via the alternating direction method of multipliers. *Foundations and Trends in Machine Learning*, 3, 1–122.

Budišić, M., Mohr, R., and Mezić, I. (2012). Applied Koopmanism. *Chaos: An Interdisciplinary Journal of Nonlinear Science*, 22, 047510.

Gaspard, P. and Tasaki, S. (2001). Liouvillian dynamics of the Hopf bifurcation. *Physical Review E*, 64, 056232.

Holmes, P., Lumley, J.L., Berkooz, G., and Rowley, C.W. (1998). *Turbulence, coherent structures, dynamical systems and symmetry*. Cambridge university press.

Lütkepohl, H. (2005). *New introduction to multiple time series analysis*. Springer Science & Business Media.

Mezič, I. (2013). Analysis of fluid flows via spectral properties of the Koopman operator. *Annual Review of Fluid Mechanics*, 45, 357–378.

Proctor, J.L., Brunton, S.L., and Kutz, J.N. (2014). Dynamic mode decomposition with control. *arXiv preprint arXiv:1409.6358*.

Rowley, C.W., Mezić, I., Bagheri, S., Schlatter, P., and Henningson, D.S. (2009). Spectral analysis of nonlinear flows. *Journal of Fluid Mechanics*, 641, 115–127.

Schmid, P.J. (2010). Dynamic mode decomposition of numerical and experimental data. *Journal of Fluid Mechanics*, 656, 5–28.

Tu, J.H., Rowley, C.W., Luchtenburg, D.M., Brunton, S.L., and Kutz, J.N. (2014). On dynamic mode decomposition: theory and applications. *Journal of Computational Dynamics*, 1, 391 – 421.

Van Leemput, P., Lust, K., and Kevrekidis, I.G. (2005). Coarse-grained numerical bifurcation analysis of lattice Boltzmann models. *Physica D: Nonlinear Phenomena*, 210, 58–76.

Williams, M.O., Rowley, C.W., and Kevrekidis, I.G. (2015a). A kernel-based approach to data-driven Koopman spectral analysis. *arXiv preprint arXiv:1411.2260*.

Williams, M.O., Kevrekidis, I.G., and Rowley, C.W. (2015b). A data-driven approximation of the Koopman operator: extending dynamic mode decomposition. *Journal of Nonlinear Science*, 25, 1307–1346.

Yuan, M. and Lin, Y. (2006). Model selection and estimation in regression with grouped variables. *Journal of the Royal Statistical Society: Series B (Statistical Methodology)*, 68, 49–67.